TENSOR DISTRIBUTION FUNCTION

Alex D. Leow and Siwei Zhu

University of California, Los Angeles, CA, USA

ABSTRACT

Diffusion weighted MR imaging is a powerful tool that can be employed to study white matter microstructure by examing the 3D displacement profile of water molecules in brain tissue. By applying diffusion-sensitizing gradients along a minimum of 6 directions, second-order tensors can be computed to model dominant diffusion processes. However, it has been shown that conventional DTI is not sufficient to resolve crossing fiber tracts. More recently, High Angular Resolution Diffusion Imaging (HARDI) seeks to address this issue by employing more than 6 gradient directions. In this paper, we introduce the Tensor Distribution Function (TDF), a probability function defined on the space of symmetric and positive definite matrices. Here, fiber crossing is modeled as an ensemble of Gaussian diffusion processes with weights specified by the TDF. Once this optimal TDF is determined, ODF can easily be computed by analytic integration of the resulting displacement probability function. Moreover, principal fiber directions can also be directly derived from the TDF.

1. INTRODUCTION

In the past decade, diffusion magnetic resonance imaging (MRI) has become a powerful tool in studying the structure of fibrous materials. By applying diffusion sensitizing gradients, diffusion MRI characterizes particle diffusivity profile in various tissues. When the duration of the applied diffusion sensitization δ is much smaller than the time between the two pulses, the MR signal attenuation is related to the displacement probability function using a Fourier integral relationship with respect to a wave vector q [1].

In brain imaging, diffusion MRI is particularly advantageous over conventional non diffusion-weighted MRI due to its ability to reveal the configuration and orientation of fiber tracts in white matter. The Diffusion Tensor MRI (DT-MRI) proposed in [2] models water displacement probability function using a zero-mean Gaussian distribution whose covariance matrix, a second-order positive symmetric tensor, thus represents the shape of local fiber tracts. Although extremely powerful and easy to compute, DT-MRI is not without it's disadvantages. For example, any Gaussian probability distribution function has only one orientational mode, and thus can not resolve fiber crossing.

More recently, High angular resolution diffusion imaging (HARDI) seeks to address this issue by sampling the q-space on shells with fixed radii. Methods such as the q-ball imaging technique [3], the Persistent Angular Structure (PAS) technique [4] and spherical-deconvolution techniques [5] are proposed to recover partial information of the displacement probability function, while still permitting the inference of underlying fiber orientations to be made.

In this paper, we propose a new approach, the computation of the tensor distribution function (TDF), to address fiber crossing and non-Gaussianity in diffusion MR images. By using Gaussian distributions as basis functions, we expand the unknown displacement probability function with the weights given by the TDF. It can also be viewed as a natural and probabilistic extension of multi-compartmental model. With the computation of TDF, the water displacement probability function, orientation distribution function (ODF), tensor orientation distribution (TOD), and its corresponding anisotropic properties can all be obtained through simple analytic relations.

2. THEORY

In standard diffusion weighted MRI, images are acquired using the Stejskal-Tanner pulsed gradient spin echo method. With some simplifications (rectangular pulse profiles), measured image intensites S are linked to p, the displacement probablity function of water molecules via the following Fourier transform

$$S(q) = S(0) \int p(x) \exp(iq \cdot x) dx \qquad (1)$$

here the wavenumber $q = r\delta G$, where r, δ, and G are the gyromagnetic ratio, the duration of the diffusion-sensitization, and the applied magnetic gradient vector. Without loss of generality, let us assume the constant S(0) is 1.

Assuming a simple Gaussian-diffusion one-tensor model, the displacement probability function evaluated at position x (given diffusion tensor D, and diffusion time t) is

$$p(x) = ((4\pi t)^3 \det(D))^{-\frac{1}{2}} \exp\Big(-\frac{x^t D^{-1} x}{4t}\Big) \qquad (2)$$

Thus, the measured diffusion MR image intensities in this one-tensor case is simply $S(q) = \exp(-tq^t Dq)$. Often times,

it is also useful to use the normalization $\tilde{q} = q/|q|$, and the notation $b = t|q|^2$. In this case, we have $S(\tilde{q}) = \exp(-b\tilde{q}^t D\tilde{q})$.

2.1. Tensor Distribution Function

Let us first denote the space of symmetric positive definite 3-by-3 matrices as $\mathbb{D}$. We seek an probablistic ensemble of tensors, as reprented by a Tensor Disribution Function P defined on the tensor space $\mathbb{D}$, that best explains the observed diffusion-weighted images. In this case, the calculated image intensity is

$$S_{calculated}(q) = \int_{D\in\mathbb{D}} P(D)\exp\Big(-tq^tDq\Big)dD \qquad (3)$$

To solve an optimal TDF P^*, we apply multiple diffusion-sensitizing directions q_is, and arrive at P^* using the least square principle

$$P^* = \text{argmin}_P \sum_i \Big(S_{obs}(q_i) - S_{calculated}(q_i)\Big)^2 \qquad (4)$$

To simplify our derivations, let us define the error vector $E(q_i) = S_{obs}(q_i) - S_{calculated}(q_i)$ to be the contribution to the total error with respect to q_i. For $P(D)$ to be a true tensor distrubtion fucntion, we have to enforce two contraints, i.e., the nonnegativtiy constraint: $P(D) \geq 0$ for every D, and the probability density constraint: $\int P(D)dD = 1$.

To enforce the first constraint, we utilize the nonnegativity property of the exponential function and let $P(D) = \exp(R(D))$. The minimization problem as proposed above is now optimized in the associated R space, thus ensuring the nonnegativity of the resulting TDF. To this end, the gradient descent in the R space for this minimization problem is thus:

$$\frac{dR}{d\tau}(D) = \sum_i 2E(q_i)\exp(R(D))F(D,q_i) \qquad (5)$$

Here, τ is an artificial time, and $F(D,q_i) = \exp\big(-tq_i^tDq_i\big)$.

Let us now turn to address the second constraint. We first rewrite this constraint in the R space: $\int_{D\in\mathbb{D}} \exp\big(R(D)\big)dD = 1$, and modify the gradient direction in Eq.(5) by gradient projection onto the constraint space. This gives us the following modified gradient descent

$$\frac{dR}{d\tau}(D) = \sum_i E(q_i)\exp(R(D))F(D,q_i) + \lambda\exp(R(D)) \qquad (6)$$

where

$$\lambda = -\frac{\int_{D\in\mathbb{D}}\exp(R(D))\sum_i E(q_i)\exp(R(D))F(D,q_i)dD}{\int_{D\in\mathbb{D}}\exp(R(D))^2dD}$$

2.2. Parametrizing Tensor Space $\mathbb{D}$

The solution space $\mathbb{D}$ is a 6 dimensional space, and some reduction is necessary for numerical optimization purposes. To this end, we assume that two eigenvalues (out of three) are equal for each individual tensor in $\mathbb{D}$. With this assumption, we only need to specify, for each tensor, one unit direction on the sphere which we associate with the third eigenvalue. Thus, each tensor is now represented by two scalars (specifying 3 eigenvalues) and one unit direction, allowing us to reduce $\mathbb{D}$ to a 4-dimentsional space. In other words, every diffusion tensor D can be expressed using $D(\lambda,\theta)$, where the eigenvalues $\lambda = (\lambda_1,\lambda_2)$ (with λ_2 the repeated eigenvalue), and $\theta = (\theta_1,\theta_2)$ the azimuthal and polar angles associated with λ_1. Notice that here we do not specify whether the two equal eigenvalues are larger or lesser compared to the third eigenvalue, thus allowing more types of tensors to be included.

Lastly, the unit direction associated with each tensor in $\mathbb{D}$ is initially expanded and parameterized with respect to the n diffusion-sensitizing gradient directions q_is. The rationale behind this particular discretization is that the angular resolution of computed fiber tracts should be linearly correlated with the number of diffuson-sensitzing gradients employed when acquiring HARDI. Once an initial solution is computed for the tensor distribution function, we further refine the angular resolution (beyond that given by the diffusion-sensitizing gradient directions) by using a multi-resolution scheme.

2.3. From TDF to ODF and Beyond

Once the optimal TDF is calculated, the displacement probabilty function p is simply:

$$p(x) = \int_{D\in\mathbb{D}} P(D)((4\pi t)^3\det(D))^{-\frac{1}{2}}\exp\Big(-\frac{x^tD^{-1}x}{4t}\Big)dD \qquad (7)$$

Moreover, the ODF can be analytically computed by radial integration:

$$ODF(\tilde{x}) = C\int_{r=0}^{\infty} p(r\tilde{x})dr$$

$$= C\int_{D\in\mathbb{D}} P(D)\Big(\det(D)\tilde{x}^tD^{-1}\tilde{x}\Big)^{-\frac{1}{2}}dD \qquad (8)$$

Here C is a normalizing constant. Lastly, we determine dominant fiber directions by examing the peaks in the Tensor Orientation Distribution Function (TOD), the marginal density function of TDF by integrating out the eigenvalues $\lambda = (\lambda_1,\lambda_2)$:

$$\text{TOD}(\theta) = \int_{\lambda} P(D(\lambda,\theta))d\lambda \qquad (9)$$

Here, we note that computing TOD may be advantageous when comparing our TDF approach to methods such as Q-ball imaging, where determination of dominant fiber tract directions is less straightforward.

3. RESULTS

In this section, we present experimental results to validate the proposed TDF approach. Two diffusion-sensitizing gradient protocols are used. The first protocol utilizes 27 diffusion-sensitizing gradient directions, evenly distributed on the hemisphere, and three baseline scans with no diffusion sensitization (i.e., T2 images), while the second protocol has 94 diffusion-sensitizing gradient directions, and 10 baseline scans with no gradient sensitization. To assess the performance of the TDF approach, we first simulate various configurations of one-tensor systems using different b values and signal-to-noise ratios (SNR) (similar to those seen in real HARDI data). In order to quantitatively compare the proposed TDF approach to other methodologies in the literature, we compare the calculated ODF (from the computed TDF) and the true ODF using L1 norm, L2 norm, and the Kullback-Leibler distance. Here, we chose $\lambda_1 = 18$ and $\lambda_2 = 2$ ($10^{-10} m^2 s^{-1}$) as the eigenvalues for each individual tensor, and employed Rician noise in our simulations. ODF is rendered using 642 points, as determined using an icosahedral approximation of the sphere.

Table 1 compares the mean and standard deviation of the three performance measures with a fixed b value and different SNR's (10, 15, and 20) using the 27-direction protocol. The results indicated that the TDF approach is robust, and is relatively independent of the level of SNR. Moreover, the results are comparable to those reported in [5]. In tables 2 and 3, we investigated the influence of b values on the performance measures, and the results indicated that the TDF approach, similar to other methodologies, performs better with increasing b values (in this paper, b ranges from 1000 to 4000 s/mm^2). To assess the performance in resolving fiber-crossing, we simulated two-tensor systems with equal weights and varying angles of crossing (45, 60 and 90 degrees), and the corresponding performances measures are shown in tables 4. Typical examples of recovered ODF's are shown in figure 1.

Similar simulations of fiber crossings were conducted using the 94-direction protocol. Interestingly, our results indicate that the 27-direction protocol performs comparable to the 94-direction protocol, indicating the numerical stability of the TDF approach.

In the next experiment, we investigate the concept of tensor orientation distribution function (TOD) by simulating 2-tensor systems with 90-degree crossing using the 94-direction protocol (the two tensors are: $10^{-10} diag(18, 2, 2) m^2 s^{-1}$ and $10^{-10} diag(2, 18, 2) m^2 s^{-1}$). Examples of computed TOD's are plotted at the bottom of Figure 1. Visually, we observe that the recovered TOD has two peaks corresponding to the true fiber orientations. To help visualize the recovered ODF's, two fiber bundles crossing at 90 degrees were simulated, using similar parameter settings as above, in a 10 by 10 by 1 grid (Figure 2, top left), notice that the fiber crossing is visually clearly resolved. In this case, the mean angular separation of the two recovered tensors, as computed using the corresponding TOD's, is 89.8 degrees with a standard deviation of 4.30 degrees.

To validate the TDF approach using real imaging data, the diffusion-weighted MR images of a normal control subject were acquired. Two regions are used: region one covers crossing of corona radiata and corpus callosum; region two is obtained from the fanning of the arcuate fascicle. The results are shown in Fig. 2. Notice that in these cases, the recovered ODF plots appear consistent with known anatomical structures.

Table 1. Mean and standard deviation (in parenthesis) of the three performance measures for one tensor simulation results with varying SNR, $b = 1200 s/mm^2$

SNR	10	15	20
KL	.0020 (1.1e-4)	.0022 (1.0e-4)	.0023 (6.2e-5)
L1	7.6e-4 (1.7e-5)	8.2e-4 (1.8e-5)	8.8e-4 (1.9e-5)
L2	.0032 (9.5e-5)	.0034 (3.5e-5)	.0035 (3.1e-5)

Table 2. Mean of the three performance measures for one tensor simulation results with varying b, SNR = 15

b	1000	1500	2000	2500	3000	3500	4000
KL	0.0022	0.0022	0.0021	0.0019	0.0018	0.0014	0.0013
L1	8.2e-4	8.2e-4	7.6e-4	7.6e-4	7.0e-4	6.4e-4	5.7e-4
L2	0.0034	0.0034	0.0033	0.0032	0.0030	0.0027	0.0026

Table 3. Estimated standard deviation of the three performance measures for one tensor simulation results with varying b, SNR = 15

b	1000	1500	2000	2500	3000	3500	4000
KL	1.2e-4	5.2e-5	8.7e-5	7.8e-5	7.9e-5	2.2e-4	1.4e-4
L1	6.4e-5	6.3e-4	6.0e-4	6.0e-4	5.5e-4	5.9e-5	3.9e-5
L2	1.1e-4	3.5e-5	7.1e-5	7.0e-5	7.2e-5	2.1e-4	1.4e-4

Table 4. Mean (and standard deviation) of the three performance measures for two tensor simulation results with varying angles, $b = 1200 s/mm^2$, SNR = 15

Angle	45	60	90
KL	2.51e-3 (2.21e-4)	3.75e-3 (5.72e-4)	3.12e-3 (4.21e-4)
L1	4.89e-4 (2.66e-5)	5.62e-4 (3.39e-5)	5.28e-4 (3.39e-5)
L2	2.08e-2 (5.44e-3)	3.70e-3 (2.82e-4)	1.27e-2 (1.60e-3)

4. CONCLUSION

In this paper, we introduced the computation of Tensor Distribution Function (TDF) as a novel methodology to resolve intravoxel fiber crossing in HARDI. We presented mathematical formulations of TDF, and proposed a projected gradient descent algorithm for the numerical computation of TDF. With minor constraints on the diffusion process and the anisotropy of individual tensors, the proposed approach solves for an underlying tensor ensemble that best describes

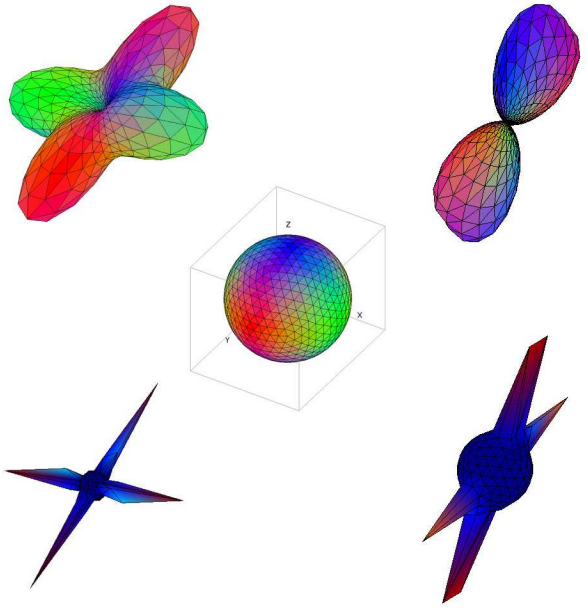

Fig. 1. **Top:** Examples of typical recovered ODFs of two-tensor system at 90 (left), and 60 (right) degrees (simulated data with 94 diffusion-sensitizing gradients, $b = 1200 s/mm^2$, and SNR = 15). In these examples, we used the multi-grid method to refine angle resolution beyond the original 94 directions. Here, the final angle resolution is given by an icosahedral approximation of the sphere (642 directions). **Center:** A sphere showing the directional color coding used for the ODFs. **Bottom:** Recovered TOD of the same 2 systems.

the observed diffusion-weighted MR images. Moreover, it is advantageous over other methodologies since displacement probability function, orientation distribution function, and principal fiber directions (or tensor orientation function) can all be directly derived from TDF through simple analytic relations.

5. REFERENCES

[1] Stejskal, E. O. and Tanner, J. E. "Spin diffusion measurements: spin echoes in the presence of a time-dependent field gradient." *J. Chem. Phys.* 42, 288-292, 1965

[2] Basser, P. J. "Inferring microstructural features and the physiological state of tissues from diffusion-weighted images." *NMR Biomed* 8, p. 333-344, 1995.

[3] Kalvis M Jansons and Daniel C Alexander. "Persistent Angular Structure: New Insights from Diffusion Magnetic Resonance Imaging Data." *Inverse Problems* 19, p. 1031-1046, 2003.

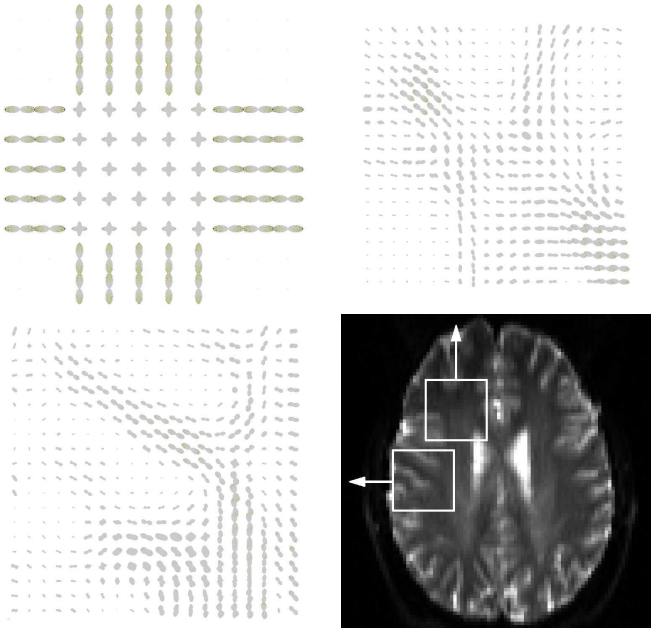

Fig. 2. **Top Left:** Recovered ODFs of a simulated 90 degrees fiber crossing with Rician noise (SNR = 15). **Top Right and Bottom Left:** Recovered ODFs from real imaging data. **Bottom Right:** Positions of the windowed areas in the patient brain. Refer to text for more information

[4] J-Donald Tournier, Fernando Calamante, David Gadian, and Alan Connelly. "Robust Determination of the Fiber Orientation Distribution in Diffusion MRI: Non-negativity Constrained Super-resolved Spherical Deconvolution." *NeuroImage* 35, p. 1459-1472, 2007.

[5] David S. Tuch. "Q-Ball Imaging." *Magnetic Resonance in Medicine* 52, p. 1358-1372, 2004.